Crossover of exciton-photon coupled modes in finite system

Motoaki Bamba[1,*] and Hajime Ishihara[2]

[1]*Department of Materials Engineering Science, Graduate School of Engineering Science, Osaka University, Toyonaka, Osaka 560-8531, Japan* [†]

[2] *Department of Physics and Electronics, Graduate School of Engineering, Osaka Prefecture University, Sakai, Osaka 599-8531, Japan*

(Dated: July 11, 2009)

An exciton and a photon behave as a polariton in macroscopic materials, while they can be treated almost independently in nano-structured ones. We have theoretically investigated the crossover of exciton-photon coupled modes, each of which is characterized with a resonance frequency and a radiative decay rate, in a semiconductor film by continuously increasing the thickness. The resonance frequency and the radiative decay rate are calculated from poles of exciton correlation functions renormalizing the exciton-photon interaction in the film, and we also introduce an intuitive calculation method with considering additional boundary conditions in order to derive the crossover condition. The general properties of the coupled modes are analytically discussed by the intuitive method.

PACS numbers: 76.20.+q, 78.67.-n, 71.35.-y, 71.36.+c

I. BACKGROUND

In order to obtain a strong and coherent response from nonlinear optical process in condensed matter, the radiative decay of elementary excitations should generally be rapid as compared to dephasing processes at their resonance conditions. The dephasings can usually be suppressed in low dimensional systems owing to the quantization of the excitation and phonon states. Especially in quantum-dot systems, very long dephasing times of subnanosecond[1,2] and more[3,4] have been experimentally observed. On the other hand, there is an attempt to enhance the radiative decay due to the strong coupling between the elementally excitation and the radiation field. In particular, the exciton superradiance, a size enhancement of the radiative decay rate of excitons, has been studied theoretically and experimentally for more than 20 years.[5–18] In a crystal where the center-of-mass motion of excitons is confined, their radiative decay rate gets larger with increasing the crystal size because of the expansion of interaction volume between the exciton and the radiation field.[5–12] The same kind of enhancement occurs with respect to the oscillator strength and nonlinearity of excitons.[6–8,19] In the case of a semiconductor film, the radiative decay rate of the lowest center-of-mass motion state of excitons gets larger with increasing thickness until about a half light wavelength at the resonance frequency, but after that it reversely decreases. The origin of this superradiance suppression is the phase mismatch between the center-of-mass motion and the radiation field.[11,12,14] In the same manner, the decay rate of the higher center-of-mass motion state is maximized at each phase-matching thickness, and the maximum value increases together with thickness in line with the exciton superradiance.[13,15–18,20–22] Further, the resonance frequency of the exciton state is also shifted due to the exciton-photon interaction,[13–18,20–22] and its anomalous frequency shift has been experimentally observed in the nondegenerate two-photon excitation scattering in a CuCl film with thickness of several tens of nanometers.[23] On the other hand, in addition to the frequency shift, a rapid decay time of about 100 fs has been observed in the degenerate four-wave mixing in a CuCl film with thickness of a several hundreds of nanometers,[24] and this is considered as the radiative decay enhanced by the exciton superradiance. Although it is usually considered that the size enhancement of the radiative decay rate is suppressed due to the dephasing processes of excitons, this suppression picture is invalid when the radiative decay rate is enhanced beyond any dephasing processes in a single crystal with few impurities and few defects as the samples used in Ref. 24. Therefore, there should be another mechanism to suppress the exciton superradiance without considering any dephasing processes.

As an answer for this question, Knoester[11] predicted and Björk et al.[13] theoretically demonstrated that the exciton superradiance is only maintained until a particular film thickness, and thereafter the radiative decay rate of the phase-matching exciton is inversely proportional to the thickness in the same manner as the radiative decay scheme of polaritons, where the decay time is proportional to the time of flight (thickness divided by group velocity).[14,25,26] Further, Björk et al. also indicated that the superradiance suppression can be interpreted as a crossover of the exciton-photon coupled modes from exciton-like (superradiant) and photon-like modes to the upper and lower branch polaritons. This is similar to the case of the cavity quantum electrodynamics (QED).[27] In the weak coupling regime between an excitation state and a cavity mode, the spontaneous emission rate is larger than the coupling strength, and these modes are slightly modified from the bare states and almost independent. On the other hand, in the strong coupling regime, the coupling strength is larger than the emission rate, and the energies of the coupled modes split into upper and lower sides (Rabi splitting). In the discussion of the exciton

superradiance, the exciton- and photon-like modes correspond to the weak-coupling regime, and a photon created by the exciton-photon recombination can go outside of the film without the reabsorption. Then, the radiative decay rate is enhanced obeying Fermi's golden rule. On the other hand, the polariton modes correspond to the strong coupling regime, and the photon is reabsorbed in the material because of the strong coupling. Therefore, the exciton and photon behave as a polariton, and the radiative decay rate is inversely proportional to the film thickness. It is known that the crossover between weak- and strong-coupling is also caused by incoherent damping,[28–30] such as exciton-phonon and exciton-exciton interactions. While this crossover and the cavity QED have a close relation with the crossover of exciton-photon coupled modes in finite system, it should be noted that the exciton-photon interaction is the origin of both the coupling and the damping in the discussion on the present paper.

However, in the calculation by Björk et al.,[13] they considered the retarded interaction (interaction via the radiation field) between the same exciton states but not between the different states. However, we should consider the inter-state retarded interaction to correctly derive the crossover thickness because of the strong exciton-photon coupling at the crossover. On the other hand, the inter-state retarded interaction has been considered in the works by Agranovich et al.[14] and by Ajiki.[15] Agranovich et al. properly considered the wavenumber uncertainty due to the breakdown of the translational symmetry perpendicular to the surface, and they demonstrated the smooth thickness dependence of radiative decay rate after the phase-matching thickness, in contrast to the oscillating behavior, which is obtained when we neglect the inter-state retarded interaction.[13,20] Further, the authors showed a correct expression of the radiative decay rate in the polariton scheme as seen in Eqs. (35) and (32) on the present paper. On the other hand, Ajiki discussed the crossover in a spherical semiconductor with a size of from quantum dot to bulk limit, and showed that the radiative decay rate decreases with increasing the crystal size if the crystal becomes larger than a particular size. The crossover condition and the size dependence of the exciton-photon coupled modes in a spherical semiconductor have been discussed in detail by Nikolaev et al.[17]

Most recently, in our previous letter,[18] we explicitly derive the crossover condition from exciton-/photon-like modes to polariton ones, and it is considered as a general condition applicable not only to a film but also to a sphere, multiple layers, photonic crystal, and so on. While this crossover condition was derived from an intuitive method based on a dispersion relation and a self-sustaining condition for the coupled modes, it should be more generalized to introduce the spatial dispersion, which originates from the center-of-mass motion of excitons. Introducing the spatial dispersion is important for the comprehensive understanding of the exciton-photon coupled modes in actual materials in experiments. Especially, its effects explicitly appear as the center-of-mass confinement of excitons in nanostructured materials,[31,32] and also in macroscopic systems as a propagation mode emerging in the polariton band gap. Further, in mesoscopic systems, it has been experimentally confirmed that the microscopic electrodynamics of excitons at interfaces is essential to explain the optical responses from such systems.[31,33,34] In addition, the large nonlinearity[35,36] and the anomalous level structure of excitons[23] were successfully explained by the microscopic nonlocal theory.[37] Nowadays, the crossover problem becomes an experimental reality due to the recent report of the rapid radiative decay in a CuCl thin film[24] as mentioned above. This material is a typical system with spatial dispersion.

One purpose of this paper is to discuss the above mentioned generalization of our previous method,[18] which is greatly helpful to link the present theory with recent experimental studies of optical response in the crossover regime. Here, we present a detailed discussion of how we can derive the equation of self-sustained condition, wherein the additional boundary conditions (ABCs)[38,39] are used to consider the spatial dispersion. As another purpose of this paper, by using the generalized method, we discuss not only the crossover of the radiative decay rate, but also the comprehensive behavior of the coupled modes, for example, the crossover of the resonance frequency, the upper limit of the radiative decay rate, the effect of spatial dispersion, and so on. These discussions will be required for the experimental verification of the crossover in the future, and also for proposing suitable material structure for strong and coherent nonlinear optical responses.

First, we explain the calculation method based on correlation function of excitons in Sec. II, and show the thickness dependence of resonance frequencies and radiative decay rates of the exciton-photon coupled modes in Sec. III. Next, we explain the intuitive method based on dispersion relation and self-sustaining condition in Secs. IV and V, respectively. In Sec. VI, we discuss the exciton-photon coupled modes in exciton-/photon-like and polariton schemes. The crossover condition of the coupled modes is derived in Sec. VII, and the general properties are shown in Sec. VIII. Last, we summarize the discussion in Sec. IX.

II. CORRELATION FUNCTION METHOD

First, we explain the calculation method for resonance frequencies and radiative decay rates of exciton-photon coupled modes from exciton correlation functions in exciton-photon inhomogeneous media. We consider a material where the translational symmetry is broken in the z direction, and discuss the behavior of s-polarized exciton whose center-of-mass is confined in a finite region. We suppose a background system characterized by

dielectric function $\varepsilon_{\rm bg}(z,\omega)$, and a resonant contribution from excitons inducing a polarization $P(z,\omega)$. We consider the Hamiltonian of the whole system as

$$\hat{H} = \hat{H}_{\rm rad} + \hat{H}_{\rm ex} + \hat{H}_{\rm int}. \tag{1}$$

Here, $\hat{H}_{\rm rad}$ represents the radiation field and the background dielectric medium, and it provides the Maxwell wave equation with quantum fluctuation as discussed in the QED of dispersive and absorptive media.[40–42] $\hat{H}_{\rm ex}$ describes the resonant contribution from excitons, and $\hat{H}_{\rm int}$ represents the interaction between the exciton and the radiation field as

$$\hat{H}_{\rm int} = -\int {\rm d}z\ \hat{E}(z)\hat{P}(z), \tag{2}$$

where $\hat{E}(z)$ is the electric field. As discussed in chap. 6 of Ref. 43, the Green's function satisfying

$$\left[(\partial^2/\partial z^2) + q^2(z,\omega)\right] G(z,z',\omega) = \delta(z-z') \tag{3}$$

corresponds to the retarded correlation function of $\hat{E}$:

$$\mu_0\omega^2 G(z,z',\omega) = \frac{1}{{\rm i}\hbar}\int_0^\infty {\rm d}t\ {\rm e}^{{\rm i}\omega t}\left\langle[\hat{E}_0(z,t),\hat{E}_0(z',0)]\right\rangle_{\rm rad}, \tag{4}$$

where the time representation of the electric field is defined as

$$\hat{E}_0(z,t) \equiv {\rm e}^{{\rm i}\hat{H}_{\rm rad}t/\hbar}\hat{E}(z){\rm e}^{-{\rm i}\hat{H}_{\rm rad}t/\hbar}. \tag{5}$$

Furthermore, under the rotating wave approximation (RWA), $G(z,z',\omega)$ also corresponds to the time-ordered correlation function of $\hat{E}$. Therefore, the correlation function of $\hat{E}$ in the background system can be obtained by finding the Green's function satisfying Eq. (3), which has already been known for general multilayer systems.[44]

Next, we discuss the time-ordered correlation functions of exciton. For simplicity, we consider only one relative motion of exciton with eigenfrequency $\omega_{\rm T}$, and denote the center-of-mass motion by index m, its annihilation operator by $\hat{b}_m$, and its eigenfrequency by Ω_m, which includes the center-of-mass kinetic energy. In the present paper, we simply consider that the exciton is a pure boson, and the system is linear as

$$\hat{H}_{\rm ex} = \sum_m \hbar\Omega_m \hat{b}_m^\dagger \hat{b}_m. \tag{6}$$

Here, the excitonic polarization appearing in Eq. (2) is quantized as

$$\hat{P}(z) = \mathcal{P}\sum_m g_m(z)\ \hat{b}_m + {\rm H.c.}, \tag{7}$$

where $g_m(z)$ is the exciton center-of-mass wavefunction in state m, and the absolute value of the coefficient $\mathcal{P}$ can be estimated by the longitudinal-transverse (LT) splitting energy of excitons as $\hbar\omega_{\rm LT} = |\mathcal{P}|^2/\varepsilon_{\rm bg}\varepsilon_0$. The self-energy tensor $\mathbf{\Sigma}(\omega)$ of exciton states is derived from the interaction Hamiltonian [Eq. (2)] as

$$\Sigma_{m,m'}(\omega) = \varepsilon_{\rm bg}\omega_{\rm LT}(\omega/c)^2 \times \int_{-\infty}^{\infty}{\rm d}z\int_{-\infty}^{\infty}{\rm d}z'\ g_m^*(z)G(z,z',\omega)g_{m'}(z'), \tag{8}$$

which describes the retarded interaction not only between the same exciton states ($m = m'$) but also between the different states ($m \neq m'$). Further, the time-ordered correlation function tensor $\mathfrak{G}(\omega)$ of exciton states in the whole system is derived from the Dyson equation, i.e., it is obtained as the inverse of the matrix whose elements are given as

$$[\mathfrak{G}^{-1}(\omega)]_{m,m'} = (\omega - \Omega_m)\delta_{m,m'} - \Sigma_{m,m'}(\omega). \tag{9}$$

The resonance frequency $\omega_{\rm res}$ and the radiative decay rate γ of exciton-photon coupled modes are respectively obtained from the real and imaginary parts of poles $\tilde{\omega} = \omega_{\rm res} - {\rm i}\gamma$ of the exciton correlation function tensor. The calculation of these poles is just identical to that of the self-sustaining modes discussed under the microscopic nonlocal theory in the semiclassical framework.[15,16,21,22,37]

The above calculation method can consider the interstate retarded interaction through the self-energy tensor, Eq. (8). Further, in the present paper, we numerically calculate the poles without any pole approximations in contrast to Ref. 15. With regard to the RWA, it can be considered as a good approximation, because neither the frequency shift nor the radiative decay rate reaches only a few percent of the bare exciton frequency $\omega_{\rm T}$ even at the maximum in the calculation.

we consider a CuCl film with thickness d, and suppose the background dielectric constant $\varepsilon_{\rm bg} = {n_{\rm bg}}^2 = 5.59$ inside of the film. In the case that the background is a homogeneous medium [$\varepsilon_{\rm bg}(z) = \varepsilon_{\rm bg}$], the Green's function satisfying Eq. (3) is derived as

$$G(z,z',\omega) = \frac{{\rm e}^{{\rm i}q|z-z'|}}{{\rm i}2q}. \tag{10}$$

On the other hand, as shown in Ref. 44, in general multilayer systems, the Green's function from a focusing layer to the same one is written as

$$\begin{aligned}&{\rm i}2qG(z,z',\omega)\\ &= {\rm e}^{{\rm i}q|z-z'|} + {\rm e}^{{\rm i}qz}\tilde{R}_L\left[{\rm e}^{{\rm i}qz'} + {\rm e}^{{\rm i}qd}\tilde{R}_R{\rm e}^{{\rm i}q(d-z')}\right]\tilde{M}\\ &\quad + {\rm e}^{-{\rm i}q(z-d)}\tilde{R}_R\left[{\rm e}^{{\rm i}q(d-z')} + {\rm e}^{{\rm i}qd}\tilde{R}_L{\rm e}^{{\rm i}qz'}\right]\tilde{M},\end{aligned} \tag{11}$$

where we consider that the left-hand interface of the focusing layer is at $z = 0$, and the right-hand at $z = d$. In Eq. (11), $\tilde{R}_{L/R}$ is the generalized reflection coefficient[44] from the focusing layer to the left-/right-hand interface,

and $\tilde{M} = [1 - \tilde{R}_L \tilde{R}_R \mathrm{e}^{\mathrm{i}2qd}]^{-1}$. In the case of a three-layer system where the background dielectric constants are respectively given as ε_L, $\varepsilon_{\rm bg}$, and ε_R, when we focus on the middle layer, $\tilde{R}_{L/R}$ is simply represented as the Fresnel reflection coefficient:

$$\tilde{R}_{L/R} = \frac{q - k_{L/R}}{q + k_{L/R}}, \tag{12}$$

where $k_{L/R}$ is the wavenumber in the left-/right-hand region:

$$k_{L/R} = \left[\varepsilon_{L/R}\omega^2/c^2 - {k_\parallel}^2\right]^{1/2}. \tag{13}$$

In the present paper, we discuss only the modes perpendicular to the layers, i.e., $k_\parallel = 0$, and we consider the wavefunctions of the exciton center-of-mass motion as sinusoidal functions whose amplitudes are zero at the interfaces of the focusing layer:

$$g_m(z) = \begin{cases} \sqrt{2/d}\sin(k_m z) & 0 < z < d \\ 0 & \text{otherwise} \end{cases} \tag{14}$$

where $k_m = m\pi/d$ and $m = 1, 2, \ldots$. The exciton translational mass is $m_{\rm ex} = 2.3 m_0$, where m_0 is the free electron mass. The bare exciton frequencies are given as $\hbar\omega_{\rm T} = 3.2022$ eV and $\Omega_m = \omega_{\rm T} + \hbar {k_m}^2/2m_{\rm ex}$. The LT splitting energy is $\hbar\omega_{\rm LT} = 5.7$ meV.

III. THICKNESS DEPENDENCE

First, we discuss the thickness dependence of the exciton-photon coupled modes in the case of homogeneous background, i.e., $\varepsilon_L = \varepsilon_R = \varepsilon_{\rm bg}$. In Fig. 1, we plot the radiative decay rate γ and resonance frequency $\omega_{\rm res}$ of the exciton-photon coupled modes with continuously changing thickness d. As seen in Fig. 1(a), γ of the lowest mode is maximized at thickness about 50 nm. Although this thickness should be approximately equal to $\lambda/2 = \pi c/n_{\rm bg}\omega_{\rm T} \simeq 80$ nm, a half light wavelength at frequency $\omega_{\rm T}$ in the background medium, we can find disagreement due to the deviation of the lowest center-of-mass motion from a continuous wave. On the other hand, in the case of the higher modes, the phase-matching condition, $k_m = m\pi/d = n_{\rm bg}\omega_{\rm T}/c$ or $d = m\lambda/2 \simeq m \times 80$ nm, is gradually satisfied with increasing the mode number because of the continuity of wavefunction increases. Further, increasing the mode number, the maximum value of γ also gets larger in line with the exciton superradiance. As theoretically demonstrated by Agranovich et al.,[14] we can find no oscillation in the thickness dependence of γ after the phase-matching thickness owing to the consideration of the inter-state retarded interaction. With regard to the resonance frequency $\omega_{\rm res}$ as seen in Fig. 1(c), when we focus on a particular mode, $\omega_{\rm res}$ gradually decreases with increasing d until the phase-matching thickness, but it flips to the higher side around its thickness. After that, $\omega_{\rm res}$ gradually decreases and saturates to $\omega_{\rm T} + \omega_{\rm LT}$, the band edge of the upper polariton. This behavior can be understood by considering the polariton dispersion relation[14,23] and the decrease of wavenumber $k_m = m\pi/d$ with increasing thickness as will be seen in Fig. 3(a).

On the other hand, as seen in Fig. 1(b), the exciton superradiance is suppressed at thickness over about 2 μm, although any dephasing processes are not considered in the calculation. According to the work by Björk et al.,[13] this behavior just reflects the crossover from exciton-/photon-like modes to polariton ones, i.e., the resonance frequencies are split to the upper and lower sides as seen in Fig. 1(d), and the radiative decay rates decrease inversely proportional to the thickness. However, only the exciton-like polariton modes are obtained in the numerical calculation of the previous section. In order to elucidate this crossover condition and to obtain the photon-like polariton modes, we calculate γ and $\omega_{\rm res}$ by another calculation method discussed in the next two sections.

IV. DISPERSION RELATION

The calculation of the previous section is based on the exciton correlation function tensor renormalizing the exciton-photon interaction. However, we should introduce another calculation method to eliminate the discontinuity seen in Figs. 1(b) and (d) and to analytically discuss the crossover of exciton-photon coupled modes. In this section, we approximate the self-energy tensor, Eq. (8), and try to derive a simplified equation for the complex frequency of the exciton-photon coupled modes by introducing a complex wavenumber, whose imaginary part represents the wavenumber uncertainty in finite systems.

In the homogeneous background medium, $\varepsilon_{\rm bg}(z,\omega) = \varepsilon_{\rm bg}(\omega)$, the Green's function satisfying Eq. (3) is diagonal with respect to the wavenumber as

$$\begin{aligned} G_{k,k'}(\omega) &= \frac{1}{L}\int_{-\infty}^{\infty}\mathrm{d}z\int_{-\infty}^{\infty}\mathrm{d}z'\ \mathrm{e}^{-\mathrm{i}kz}\ G(z,z',\omega)\ \mathrm{e}^{\mathrm{i}k'z'} \\ &= \frac{\delta_{k,k'}}{(q+\mathrm{i}\delta)^2 - k^2}, \end{aligned} \tag{15}$$

where L is the normalization length. Eq. (10) can be obtained by transforming this equation into the real space. Substituting Eq. (15) into Eq. (8), we obtain

$$\Sigma_{m,m'}(\omega) = \omega_{\rm LT}\ {q_0}^2 \sum_k \frac{g^*_{m,k}\ g_{m',k}}{(q+\mathrm{i}\delta)^2 - k^2}, \tag{16}$$

where ${q_0}^2 \equiv \varepsilon_{\rm bg}\omega^2/c^2$, and $g_{m,k}$ is the Fourier transform of the exciton center-of-mass wavefunction:

$$g_{m,k} = \frac{1}{\sqrt{L}}\int_{-\infty}^{\infty}\mathrm{d}z\ \mathrm{e}^{-\mathrm{i}kz} g_m(z). \tag{17}$$

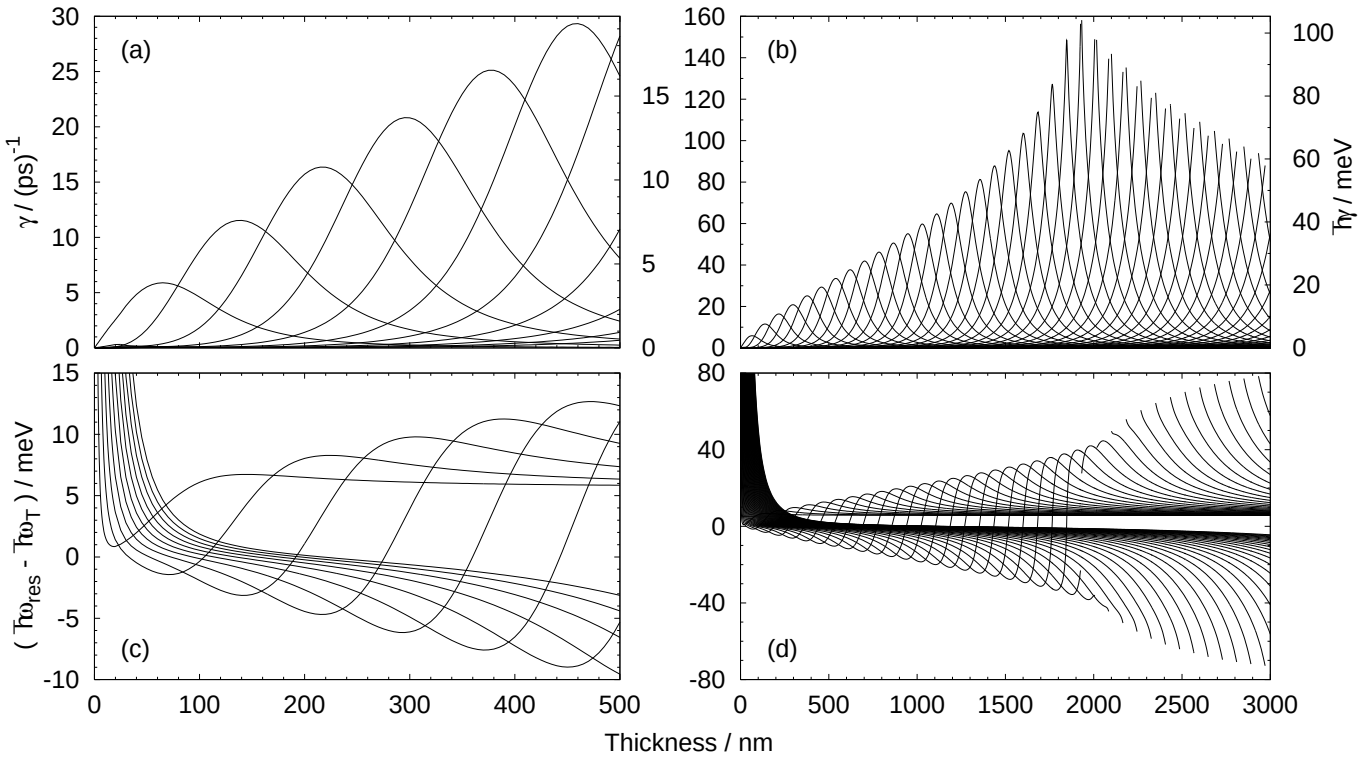

FIG. 1: (a) (b) Radiative decay rates γ and (c) (d) resonance frequency $\omega_{\rm res}$ of the exciton-photon coupled modes in a CuCl film are plotted as a function of the film thickness. (a) and (c) are, respectively, enlarged views of (b) and (d) for small thickness region. While 200 states of exciton center-of-mass motion are considered in the numerical calculation, for the sake of easy view, the values of the lowest 10 and 45 modes are plotted in (a) (c) and (b) (d), respectively. The dielectric constants of outside media are $\varepsilon_L = \varepsilon_R = \varepsilon_{\rm bg}$.

In contrast to the infinitesimal interval $2\pi/L$ between the neighboring k, the interval of q_m is much large in the order of π/d. Therefore, the base-transformation between m and k is not unitary in the case of a film with finite thickness. This means that the transform coefficient set $\{g_{m,k}\}$ satisfies the orthogonality as

$$\sum_k g^*_{m,k}\ g_{m',k} = \int_{-\infty}^{\infty} {\rm d}z\ g_m(z)\ g^*_{m'}(z) = \delta_{m,m'}, \quad (18)$$

but it does not satisfy the completeness:

$$\sum_m g^*_{m,k} g_{m,k'} = \frac{1}{L}\int_{-d/2}^{d/2} {\rm d}z\ {\rm e}^{{\rm i}(k-k')z} = \frac{d}{L}\frac{\sin[(k-k')d/2]}{(k-k')d/2}, \quad (19)$$

where we consider that the exciton center-of-mass motion is confined in $-d/2 < z < d/2$. Therefore, the self-energy, Eq. (16), becomes diagonal with respect to k only in infinite systems.

In order to obtain a simple equation for analytically discussing the exciton-photon coupled modes, we consider the following approximation to quasi-diagonalize the self-energy, Eq. (16). The function $\sin(x)/x$ appearing in Eq. (19) can be approximated as $\sin(x)/x \simeq 1$ under the condition $|x| \ll 1$. Therefore, by relaxing the identical condition of k as $|k-k'| \ll d^{-1}$, Eq. (19) can be approximated as

$$(L/d)\sum_m g^*_{m,k} g_{m,k} \simeq \delta_{k,k'}, \quad (20)$$

and then $\{g_{m,k}\}$ has a quasi-completeness. Here, since we admit an uncertainty of k in the order of d^{-1}, the wavenumber should have an imaginary part as $k \to k - {\rm i}\alpha/d$, and the summation becomes $\sum_k \to (L/d)\sum_k$. The physical meaning of the nondimensional value α will be discussed later. As the result of the above approximation, the self-energy, Eq. (16), becomes quasi-diagonal as

$$\Sigma_{k,k'}(\omega) = \sum_{m,m'} g_{m,k}\ \Sigma_{m,m'}(\omega)\ g^*_{m',k'} \simeq \frac{d}{L}\delta_{k,k'}\frac{\omega_{\rm LT}\ {q_0}^2}{(q+{\rm i}\delta)^2 - (k-{\rm i}\alpha/d)^2}. \quad (21)$$

In the same manner, the diagonal part of the correlation function, Eq. (9), is rewritten as

$$\sum_m g_{m,k}(\Omega_m - \omega) g^*_{m,k'} \simeq \delta_{k,k'}\frac{d}{L}\left[\Omega(k - {\rm i}\alpha/d) - \omega\right], \quad (22)$$

where the bare exciton frequency is written as

$$\Omega(k-\mathrm{i}\alpha/d)=\omega_{\mathrm{T}}+\frac{\hbar}{2m_{\mathrm{ex}}}\left[{k_{\parallel}}^2+\left(k-\mathrm{i}\frac{\alpha}{d}\right)^2\right]. \quad (23)$$

Therefore, the exciton correlation function can be obtained as a diagonal form as

$$[\mathfrak{G}^{-1}(\omega)]_{k,k'}=\sum_{m,m'}g_{m,k}[\mathfrak{G}^{-1}(\omega)]_{m,m'}g^{*}_{m',k'}$$
$$\simeq\delta_{k,k'}\frac{d}{L}\left[\omega-\Omega(k-\mathrm{i}\alpha/d)-\frac{\omega_{\mathrm{LT}}\ {q_0}^2}{(q+\mathrm{i}\delta)^2-(k-\mathrm{i}\alpha/d)^2}\right], \quad (24)$$

and the pole $\tilde{\omega}=\omega_{\mathrm{res}}-\mathrm{i}\gamma$ is obtained for a given complex wavenumber $\tilde{k}=k-\mathrm{i}\alpha/d$ from

$$\tilde{\omega}=\Omega(\tilde{k})+\frac{\omega_{\mathrm{LT}}\varepsilon_{\mathrm{bg}}(\tilde{\omega}/c)^2}{\varepsilon_{\mathrm{bg}}(\tilde{\omega}/c)^2-{k_{\parallel}}^2-\tilde{k}^2}. \quad (25)$$

Here, we can rewrite this into the dispersion relation

$$\frac{c^2({k_{\parallel}}^2+\tilde{k}^2)}{\tilde{\omega}^2}=\varepsilon_{\mathrm{bg}}+\frac{\varepsilon_{\mathrm{bg}}\omega_{\mathrm{LT}}}{\Omega(\tilde{k})-\tilde{\omega}}=\varepsilon_{\mathrm{bg}}+\chi(\tilde{k},\tilde{\omega}), \quad (26)$$

which has the same form as that in the bulk system. However, there remains a task to determine the nondimensional value α and the k-selection rule that governs the discrete k values for a finite thickness.

V. SELF-SUSTAINING CONDITION WITH ABC

In order to determine the complex wavenumber $\tilde{k}=k-\mathrm{i}\alpha/d$, we consider a self-sustaining condition of exciton-photon coupled modes in a film with polariton dispersion. If the translational mass of exciton is assumed to be infinite, there is only a single polariton mode satisfying dispersion relation (25) for a given frequency $\tilde{\omega}$, and the self-sustaining condition is simply considered as[18]

$$r_L\ r_R\ \mathrm{e}^{\mathrm{i}2\tilde{k}d}=1, \quad (27)$$

where $r_{L/R}$ is the Fresnel reflection coefficient at the left-/right-hand interface:

$$r_{L/R}=\frac{\tilde{k}-\tilde{k}_{L/R}}{\tilde{k}+\tilde{k}_{L/R}}, \quad (28)$$

and $\tilde{k}_{L/R}$ is the outside wavenumber defined in Eq. (13) by replacing ω with $\tilde{\omega}=\omega_{\mathrm{res}}-\mathrm{i}\gamma$. The self-sustaining condition, Eq. (27), means that there is neither amplitude decay nor phase shift after a round trip inside of the film. Actually, this intuitive method consisting of the dispersion and self-sustaining condition approximately provides the complex wavenumber set $\{\tilde{\omega}_\lambda\}$ obtained by the correlation function method.[18] However, if we discuss the exciton center-of-mass kinetic energy with finite translational mass, we usually consider ABCs[38,39] besides the Maxwell boundary conditions, because there are two wavenumbers $\tilde{k}_1$ and $\tilde{k}_2$ satisfying dispersion relation (25) for a given $\tilde{\omega}$. In the present paper, we extend Eq. (27), which was introduced in our previous letter,[18] by considering ABCs as follows.

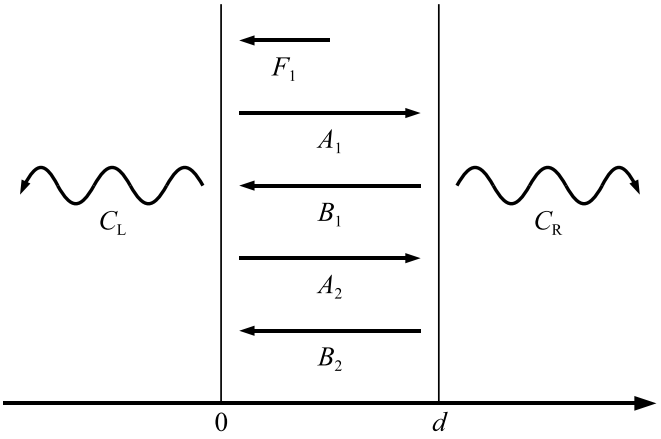

FIG. 2: Schematic view of polariton and photon fields to calculate the reflection coefficients from inside of the film. $A_{1/2}$ and $B_{1/2}$ are polariton fields with wavenumber $\tilde{k}_{1/2}$ inside the film, $C_{L/R}$ is an out-going field to left/right-hand side, and F_1 is an incident field with wavenumber k_1 from inside of the film.

As seen in Fig. 2, we consider forward (A_1 and A_2) and backward fields (B_1 and B_2) for each polariton mode, and two outward fields (C_L and C_R) from the film. In order to derive the reflection coefficients for polariton 1 from inside of the film, we consider an incident field F_1 from inside to the left interface. In the present paper, we solve this boundary problem by using Pekar's ABC,[38,45] because we consider the exciton center-of-mass wavefunction [Eq. (14)] whose amplitudes are zero at the interfaces. However, we usually cannot define the reflectance from inside of the film with multiple polariton modes, because the amplitude of one mode is also transferred to the other modes after the reflection, and it also goes back to the original mode after another reflection. In order to derive the appropriate self-sustaining condition, we should determine the reflection coefficients r'_L and r'_R in this system. Here, we consider that, as a result of the multiple reflections inside of the film, B_1/F_1 should be represented by a product of the two reflection coefficients as

$$B_1/F_1=\sum_{n=1}^{\infty}(r'_L r'_R\ \mathrm{e}^{\mathrm{i}2\tilde{k}_1 d})^n, \quad (29)$$

and, comparing with Eq. (27), the self-sustaining condition for the multimode system is obtained as

$$r'_L r'_R\ \mathrm{e}^{\mathrm{i}2\tilde{k}_1 d}=\frac{(B_1/F_1)}{1+(B_1/F_1)}=1. \quad (30)$$

Although this equation is satisfied only in the limit of $|B_1/F_1| \to \infty$, we renew $\tilde{k}_1$ as

$$\tilde{k}_1 := \frac{-1}{\mathrm{i}2d} \ln(r'_L\ r'_R) = \frac{-1}{\mathrm{i}2d} \ln \frac{(B_1/F_1)\mathrm{e}^{-\mathrm{i}2\tilde{k}_1 d}}{1+(B_1/F_1)}. \quad (31)$$

in the numerical successive calculation. Actually, by simultaneously solving Eqs. (25) and (31), we can reproduce $\{\omega_{\rm res} - \mathrm{i}\gamma\}$ obtained by the correlation function method explained in Sec. II.

VI. COUPLED MODES IN TWO SCHEMES

In Fig. 3, we show (a) dispersion relation and (b) frequency dependence of γ at thicknesses of 50, 200, and 500 nm. The poles of the correlation functions of excitons are plotted with symbols, and $\tilde{k} = k - \mathrm{i}\alpha/d$ is calculated from dispersion relation (25) for each $\tilde{\omega} = \omega_{\rm res} - \mathrm{i}\gamma$. On the other hand, the lines are calculated for a given k by the intuitive method discussed in the previous two sections. However, we neglect the k-selection rule to show the continuous k-dependence, and the ABCs are also neglected, because the modes are obtained only at particular wavenumbers when we consider the ABCs. In other words, instead of Eq. (31), we consider only the relation between α and $\tilde{\omega}$ for a given real k as

$$\alpha = \frac{1}{4} \ln \frac{1}{|r_L r_R|^2}, \quad (32)$$

where $r_{L/R}$ is the reflection coefficient without considering the ABC, i.e., the Fresnel coefficient [Eq. (28)]. Eqs. (25) and (32) give solutions for arbitrary k as seen in Fig. 3. If the ABCs are considered, the solutions are obtained only for particular k satisfying the self-sustaining condition [Eq. (30)].

Since dispersion relation (25) is rewritten into a third-order polynomial equation for $\tilde{\omega}$ as

$$[\tilde{\omega} - \Omega(\tilde{k})][\varepsilon_{\rm bg}(\tilde{\omega}/c)^2 - {k_\parallel}^2 - \tilde{k}^2] = \omega_{\rm LT}\varepsilon_{\rm bg}(\tilde{\omega}/c)^2, \quad (33)$$

there are three solutions for a given $\tilde{k}$. One is an unphysical solution with negative frequency, and the other two satisfying Eq. (32) are plotted in Fig. 3 for a given real k. One solution has an exciton-like frequency $\omega_{\rm res} \simeq \omega_{\rm T}$ with small γ, and the other has a photon-like frequency $\omega_{\rm res} \simeq ck/n_{\rm bg}$ with large γ. These exciton-like and photon-like modes are slightly modified from the bare exciton and photon states, respectively, because of the relatively weak exciton-photon coupling in the thin film. As seen in Figs. 3(a) and (b), increasing the thickness, γ of the exciton-like mode with phase-matching ($k \simeq n_{\rm bg}\omega_{\rm T}/c$) also increases in line with the exciton superradiance, and the deviation of $\omega_{\rm res}$ from $\omega_{\rm T}$ also increases around the phase-matching wavenumber. By using the correlation function method, only the exciton-like modes are numerically obtained. This can be understood by rewriting dispersion relation (25) as

$$\tilde{\omega} - \Omega(\tilde{k}) - \frac{\omega_{\rm LT}\varepsilon_{\rm bg}(\tilde{\omega}/c)^2}{\varepsilon_{\rm bg}(\tilde{\omega}/c)^2 - {k_\parallel}^2 - \tilde{k}^2} = f(\tilde{\omega}, \tilde{k}) = 0. \quad (34)$$

It is difficult to numerically find the zero points of function $f(\tilde{\omega}, \tilde{k})$ for the photon-like solutions ($k \simeq n_{\rm bg}\omega_{\rm res}/c$), because the last term on the left-hand side (LHS) becomes divergent. Therefore, we could not numerically find the photon-like poles of the correlation function tensor of excitons [Eq. (9)]. This is the reason of the discontinuity seen in Figs. 1(b) and (d). On the other hand, although we can find good agreements between symbols and lines in the dispersion relation [Fig. 3(a)], there are some deviations of γ as seen in Fig. 3(b), especially for thickness of 50 nm and for wavenumber larger than $10 \times n_{\rm bg}\omega_{\rm T}/c$. The reason of this is the neglect of ABC in the intuitive calculation method. Instead of such an approximated treatment used in Ref. 18, by considering the ABC as explained in Sec. V, we can obtain the exact agreement between the two calculation results under the numerical precision.

As discussed by Agranovich et al.,[14] the representation of α [Eq. (32)] is also obtained along the calculation of radiative decay rate in the polariton scheme, which provides the radiative decay rate as

$$\gamma = \alpha v_{\rm g}/d. \quad (35)$$

On the other hand, in the present intuitive calculation method, Eq. (32) is obtained from the self-sustaining condition, and Eq. (35) can be obtained from dispersion relation (25) in particular situations. When the radiative decay rate is much smaller than the resonance frequency as $\gamma \ll \omega_{\rm res}$ and the uncertainty of the wavenumber is much small as $\alpha/d \ll k$, Eq. (25) can be approximated as

$$\omega = \omega_{\rm T} + \frac{\hbar k^2}{2m_{\rm ex}} + \frac{\omega_{\rm LT}\ {q_0}^2}{{q_0}^2 - {k_\parallel}^2 - k^2}, \quad (36)$$

$$\gamma = \frac{\hbar k}{m_{\rm ex}} \frac{\alpha}{d} + \frac{2\omega_{\rm LT}{q_0}^2[k\alpha/d - ({k_\parallel}^2 + k^2)\gamma/\omega]}{({q_0}^2 - {k_\parallel}^2 - k^2)^2}. \quad (37)$$

Here, Eq. (36) is just the dispersion relation in bulk system under the RWA, and it gives the group velocity in infinite system as

$$v_{\rm g} = \frac{\mathrm{d}\omega}{\mathrm{d}k} = \frac{({q_0}^2 - {k_\parallel}^2 - k^2)^2\hbar k/m_{\rm ex} + 2\omega_{\rm LT}{q_0}^2 k}{({q_0}^2 - {k_\parallel}^2 - k^2)^2 + 2\varepsilon_{\rm bg}\omega_{\rm LT}\omega({k_\parallel}^2 + k^2)/c^2}. \quad (38)$$

From this representation of $v_{\rm g}$, Eq. (35) can be obtained by rewriting Eq. (37). While the group velocity in damped system is actually represented as in Ref. 28, the above definition for non-damped system is suited for the radiative decay picture of polaritons, because it is considered that the polariton is damped only at the film

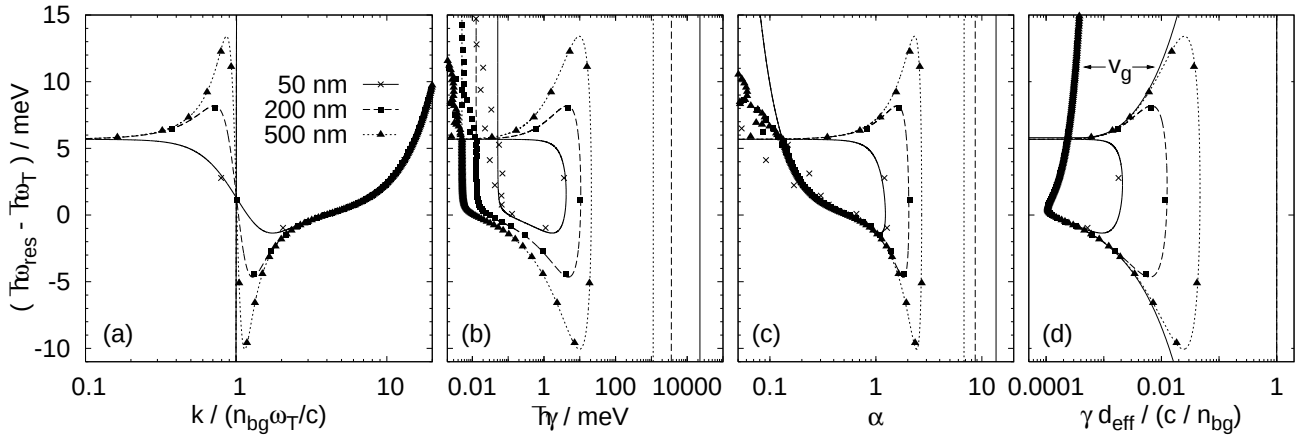

FIG. 3: (a) Wavenumber k, (b) radiative decay rate γ, (c) factor α of effective thickness $d/\alpha = -\mathrm{Im}[\tilde{k}]^{-1}$, and (d) apparent propagation speed γd_{eff} are plotted as a function of resonance frequency ω_{res} of exciton-photon coupled modes in a CuCl film with thicknesses of 50, 200, and 500 nm. The lines are calculated by solving Eqs. (25) and (32) for a given real wavenumber k, and the symbols are calculated by the correlation function method. The dielectric constants of outside media are $\varepsilon_L = \varepsilon_R = \varepsilon_{\mathrm{bg}}$.

surfaces and propagates inside the film as in the non-damped system. It is worth noting that Eq. (35) is derived without any information outside of the excitonic medium, while α itself is determined by the outside information reflected through the self-sustaining condition, Eq. (27) or (30). Although Eq. (35) cannot be applied to superradiant excitons, we define an effective thickness of an exciton-photon coupled mode as

$$d_{\mathrm{eff}} = d/\alpha = -\mathrm{Im}[\tilde{k}]^{-1}, \tag{39}$$

which gives $\gamma = v_{\mathrm{g}}/d_{\mathrm{eff}}$ in the polariton scheme. Further, we define an apparent propagation speed of the coupled modes as γd_{eff}, the effective thickness divided by the radiative decay time, and it agrees with v_{g} in the polariton scheme.

In Fig. 3(c) and (d), we respectively plot the frequency dependence of α and γd_{eff}, and also we plot the polariton group velocity v_{g} with bold solid lines in Fig. 3(d). Although γd_{eff} of superradiant excitons ($k \simeq n_{\mathrm{bg}}\omega_{\mathrm{T}}/c$ and $\omega_{\mathrm{res}} \simeq \omega_{\mathrm{T}}$) gets larger with increasing thickness, we can find that γd_{eff} of the other exciton-like modes agree with v_{g}. In other words, all the exciton-like modes without the phase-matching condition obey the polariton scheme even at small thickness where the exciton superradiance is maintained. This is because that the conditions $\gamma \ll \omega_{\mathrm{res}}$ and $\alpha/d \ll k$, which are used to derive Eq. (37), are satisfied even for those phase-mismatching modes. On the other hand, we can find that γd_{eff} of photon-like modes agree with c/n_{bg}, the light speed in the background medium, because of the relatively weak exciton-photon coupling at the small thickness. As seen in Fig. 3(c), there are some deviations of α between the two calculation methods for large wavenumber and for small thickness. This is because α is determined without considering ABCs. On the other hand, γd_{eff} of the two are well agreed even for large wavenumber, because Eq. (35) is obtained only from dispersion relation (25).

Fig. 4 shows the dispersion relation and frequency dependence of γ, α, and γd_{eff} at large thicknesses of 1.6, 2, and 3 μm. For thickness of 1.6 μm, where the exciton superradiance is maintained, γ and γd_{eff} of the superradiant modes are much larger than those in Fig. 3 obeying the exciton superradiance. On the other hand, γd_{eff} of photon-like modes are apart from c/n_{bg} because of the relatively strong exciton-photon coupling. In this thickness region near the crossover, increasing the thickness, γd_{eff} of the superradiant and photon-like modes gradually close to each other, and after the crossover of exciton-photon coupled modes, the two solutions of the intuitive method split into the upper and lower branches as seen in Fig. 4(a). After that, the phase-matching modes disappear from the polariton band gap, and then the exciton superradiance is suppressed. On the other hand, the frequency dependence of γ also splits into upper and lower branches, and γd_{eff} gradually saturates to the polariton group velocity v_{g} even at the phase-matching condition. Therefore, all the modes obey the polariton scheme after the crossover. This is the suppression mechanism of the exciton superradiance as discussed by Björk et al.[13]

VII. CROSSOVER CONDITION

As indicated in our previous letter,[18] the crossover condition between the exciton/photon-like modes and the polariton ones can be obtained from dispersion relation (25). At the phase-matching condition ${k_{\parallel}}^2 + k^2 = \varepsilon_{\mathrm{bg}}{\omega_{\mathrm{T}}}^2/c^2$, the real part of Eq. (33) is written as

$$(\omega-\omega_{\mathrm{T}})(\omega^2-\gamma^2-{\omega_{\mathrm{T}}}^2+\beta^2)-2\gamma\,[\omega\gamma-(ck/n_{\mathrm{bg}})\beta] = \omega_{\mathrm{LT}}\omega^2, \tag{40}$$

where $\beta = c\alpha/n_{\mathrm{bg}}d$. Further, at small thickness where the exciton superradiance is maintained, the resonance frequency obeys $\omega_{\mathrm{res}} \simeq \omega_{\mathrm{T}}$ as seen in Fig. 3(a), and the

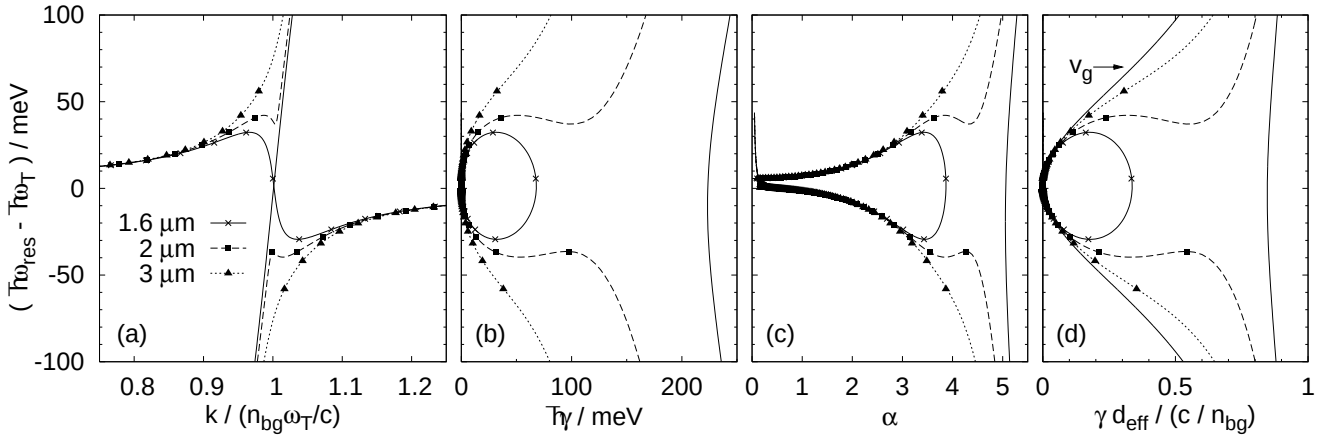

FIG. 4: (a) Wavenumber k, (b) radiative decay rate γ, (c) factor α of effective thickness $d/\alpha = -\mathrm{Im}[\tilde{k}]^{-1}$, and (d) apparent propagation speed $\gamma d_{\rm eff}$ are plotted as a function of resonance frequency $\omega_{\rm res}$ of exciton-photon coupled modes in a CuCl film with thicknesses of 1.6, 2, and 3 μm. The lines are calculated by solving Eqs. (25) and (32) for a given real wavenumber k, and the symbols are calculated by the correlation function method, where 400 states of exciton center-of-mass motion are considered in the numerical calculation. The dielectric constants of outside media are $\varepsilon_L = \varepsilon_R = \varepsilon_{\rm bg}$.

first bracket on the LHS of Eq. (40) is negligible:

$$\gamma^2 - \eta(c\alpha/n_{\rm bg}d)\gamma + \omega_{\rm T}\omega_{\rm LT}/2 = 0, \tag{41}$$

where $\eta = ck/n_{\rm bg}\omega_{\rm T}$ is the z component of the unit vector in the propagation direction. When the film is thin enough compared to the crossover thickness, the two solutions of Eq. (41) are obtained as

$$\gamma = (n_{\rm bg}\omega_{\rm T}\omega_{\rm LT}/2\eta c)d_{\rm eff} \tag{42}$$

for the exciton-like (superradiant) mode, and

$$\gamma = \eta(c/n_{\rm bg})/d_{\rm eff} \tag{43}$$

for the photon-like mode. Here, we can find that the propagation speed of the latter is the light speed $\eta(c/n_{\rm bg})$ perpendicular to the film in the background medium, and it can be seen in Fig. 3(d), where $k_\parallel = 0$ and then $\eta = ck/n_{\rm bg}\omega_{\rm T} = 1$. Since Eq. (42) is proportional to d and Eq. (43) is to d^{-1}, these two quantities gradually close to each other with increasing the thickness, and they finally reach to

$$\gamma d_{\rm eff} = \eta c/2n_{\rm bg}, \tag{44}$$

which is the degenerate solution of Eq. (41). This is the crossover condition between exciton-/photon-like modes and polariton ones, and it is roughly verified in Fig. 4(d). Since $c/2n_{\rm bg}$ is the polariton group velocity at the phase-matching wavenumber, Eq. (44) means that the crossover occurs when the apparent propagation speed $\gamma d_{\rm eff}$ of superradiant exciton reaches the group velocity $c/2n_{\rm bg}$ of polariton. Therefore, the photon created by the electron-hole recombination cannot go outside of the film without reabsorption, when its propagation speed looks beyond the group velocity. In this situation, as seen in Fig. 1(b), the radiative life time is much shorter than the inverse

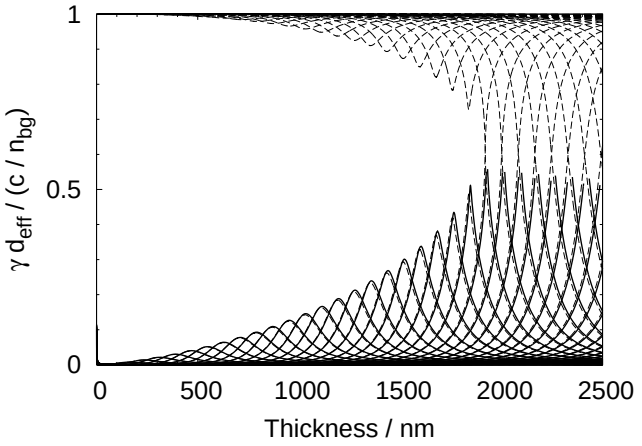

FIG. 5: Thickness dependence of apparent propagation speed $\gamma d_{\rm eff}$. Dashed lines are calculated by the intuitive method with ABC, and solid lines are by the correlation function method. 200 exciton states are considered in the latter calculation, and the small deviation at large thicknesses comes from this finiteness. The dielectric constants of outside media are

$$\varepsilon_L = \varepsilon_R = \varepsilon_{\rm bg}.$$

of the LT splitting (5.7 meV), which is the life time of exciton localized at a single ion. This enhancement is just the effect of the exciton superradiance realized under the phase-matching between the radiation field and the center-of-mass motion of exciton.

Fig. 5 shows the thickness dependence of $\gamma d_{\rm eff}$. The solid lines are calculated by the correlation function method, and the effective thickness $d_{\rm eff}$ is derived from dispersion relation (25) for each $\tilde{\omega} = \omega - {\rm i}\gamma$. On the other hand, dashed lines are calculated by the intuitive

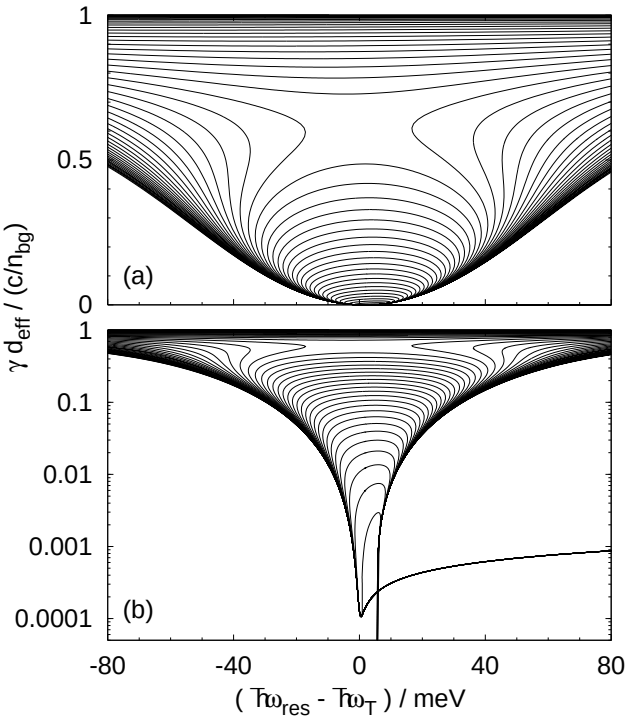

FIG. 6: Apparent propagation speeds $\gamma d_{\rm eff}$ of exciton-photon coupled modes are plotted as a function of their resonance frequencies $\omega_{\rm res}$ by changing the film thickness. The data is calculated by the intuitive method with ABC, and plotted (a) in linear scale and (b) in log scale. The dielectric constants of outside media are $\varepsilon_L = \varepsilon_R = \varepsilon_{\rm bg}$.

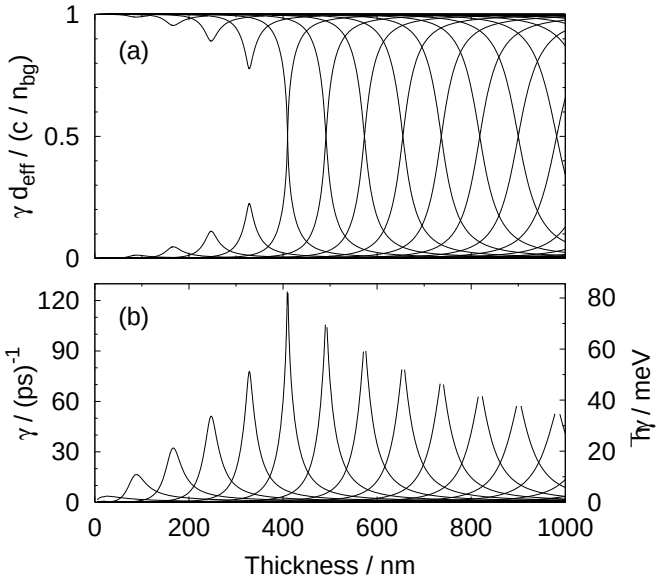

FIG. 7: (a) Apparent propagation speed $\gamma d_{\rm eff}$ and (b) radiative decay rate of exciton-photon coupled modes in a CuCl film are plotted as a function of the film thickness. The dielectric constants of outside media are $\varepsilon_L = \varepsilon_R = 1$. (a) is calculated by the intuitive method with ABC, and (b) is by the correlation function method.

method with ABC, i.e., by simultaneously solving dispersion relation (25) and self-sustaining condition (31). We can verify that the crossover occurs when $\gamma d_{\rm eff}$ of superradiant exciton reaches $c/2n_{\rm bg}$. On the other hand, Fig. 6 shows the frequency dependence of $\gamma d_{\rm eff}$ with continuously changing the thickness, and it is calculated by simultaneously solving Eqs. (25) and (31). When we focus on a particular mode with relatively small mode number, $\omega_{\rm res}$ shifts to the lower side and γ gets larger with increasing d until its phase-matching thickness, and around its thickness, $\omega_{\rm res}$ flips to the higher side with maximizing γ. After that, $\omega_{\rm res}$ decreases to the band edge $\omega_{\rm T} + \omega_{\rm LT}$ of the upper branch, and γ monotonally decreases. Although the maximum value of γ gradually increases together with d in line with the exciton superradiance, it is suppressed when $\gamma d_{\rm eff}$ reaches $c/2n_{\rm bg}$ as discussed above. After the crossover, the exciton-photon coupled modes split into upper and lower branches, and $\gamma d_{\rm eff}$ gradually decreases and saturate to the polariton group velocity $v_{\rm g}$ when we focus on a particular frequency. On the other hand, as seen in Fig. 6(b), $\gamma d_{\rm eff}$ of the phase-mismatching modes agree with $v_{\rm g}$ even at small thickness where the exciton superradiance is maintained. It is worth noting that, by using the intuitive method with ABCs on the present paper, we can obtain correct exciton-photon coupled modes under such phase-mismatching conditions, in contrast to the deviation shown in Fig. 3, which is obtained by the previous calculation method without ABCs.[18]

VIII. GENERAL PROPERTIES

It is worth to note that the breakdown condition [Eq. (44)] should be applied to general situations, for example, a excitonic layer in cavity, multiple layers separated by a transparent layer, a sphere as discussed by Ajiki,[15] and photonic crystal structures. This is because Eq. (44) is simply derived from the dispersion relation, Eq. (25), which includes no information outside of the excitonic medium. As a demonstration of the generality, we verify the breakdown condition for a CuCl film in vacuum, i.e., $\varepsilon_L = \varepsilon_R = 1$. Fig. 7 shows the thickness dependence of (a) $\gamma d_{\rm eff}$ and (b) γ. The former is calculated by the intuitive method with ABC, and the latter is by the correlation function method. As the result of the multiple reflections inside of the film, the size enhancement of γ becomes more rapid and the crossover thickness becomes smaller compared to Fig. 1, where the outside dielectric constant is $\varepsilon_L = \varepsilon_R = \varepsilon_{\rm bg}$. In other words, $d_{\rm eff} = d/\alpha$ is enhanced by the multiple reflections obeying Eq. (32). However, we can find that the breakdown also occurs when $\gamma d_{\rm eff}$ reaches $c/2n_{\rm bg}$ as seen in Fig. 7(a). On the other hand, Fig. 8 shows the frequency dependence of $\gamma d_{\rm eff}$, and it also reflects the crossover from the exciton-/photon-like modes to polariton ones as dis-

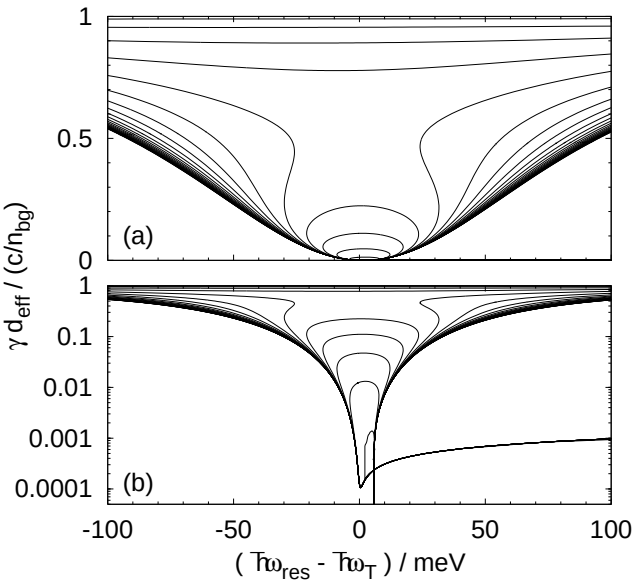

FIG. 8: Apparent propagation speeds $\gamma d_{\rm eff}$ of exciton-photon coupled modes are plotted as a function of their resonance frequencies $\omega_{\rm res}$ by changing the film thickness. The data is calculated by the intuitive method with ABC, and plotted (a) in linear scale and (b) in log scale. The dielectric constants of outside media are $\varepsilon_L = \varepsilon_R = 1$.

cussed above. It is worth noting that the crossover thickness in actual situation is in the order of several hundreds of nanometers due to the multiple reflections as seen in Fig. 7. Moreover, considering an optical cavity outside of the film, a further enhancement of the multiple reflections make the crossover thickness smaller than the phase-matching thickness (about 80 nm) of the first center-of-mass motion. In this situation, we cannot obtain the superradiant modes, and all the exciton-photon coupled modes are considered as (cavity) polaritons.

For a large thickness where the polariton scheme is valid, at the phase-matching condition $k = n_{\rm bg}\omega_{\rm T}/c$, the resonance frequencies of exciton-photon coupled modes agree with those of bulk polariton as

$$\omega \simeq \omega_{\rm T} \pm \omega_{\rm T}\sqrt{\frac{\omega_{\rm LT}}{2\omega_{\rm T}}}, \tag{45}$$

which is approximately obtained from Eq. (36). On the other hand, the crossover thickness is obtained from the condition that Eq. (41) has the degenerate solution:

$$d/\alpha = \frac{c}{n_{\rm bg}\sqrt{2\omega_{\rm T}\omega_{\rm LT}}} = \frac{\lambda}{2\pi}\sqrt{\frac{\omega_{\rm T}}{2\omega_{\rm LT}}}, \tag{46}$$

where $\lambda = 2\pi c/n_{\rm bg}\omega_{\rm T}$ is the light wavelength in the background. Therefore, the maximum value of γ of the superradiant mode is derived as

$$\gamma = \frac{c/2n_{\rm bg}}{d/\alpha} = \omega_{\rm T}\sqrt{\frac{\omega_{\rm LT}}{2\omega_{\rm T}}}. \tag{47}$$

This is just the frequency shift of bulk polariton at $k = n_{\rm bg}\omega_{\rm T}/c$ as seen in Eq. (45). For the CuCl crystal, the frequency shift is about 80 meV as seen in Fig. 4(a), and we can find the validity of Eq. (47) in Fig. 1(b) and Fig. 7(b), although larger γ is obtained for polariton modes just after the crossover, and also much larger γ is obtained for photon-like modes at small thickness. However, in order to obtain a strong and rapid nonlinear optical response, we must also consider the amount of exciton component in these exciton-photon coupled modes, and discuss the most suitable thickness that gives both large exciton nonlinearity and rapid radiative decay. From such a viewpoint, nano-structured materials around the crossover are promising for the strong and rapid nonlinear responses, because a large nonlinearity[35] and the rapid radiative decay[24] have been reported theoretically and experimentally. The intuitive method with ABC, which is introduced in the present paper, is a powerful tool to comprehensively discuss the exciton-photon coupled modes in such finite materials.

IX. SUMMARY

We have calculated the resonance frequency and the radiative decay rate of exciton-photon coupled modes in a CuCl film with finite thickness, and investigated the crossover of the coupled modes from exciton-/photon-like to polariton scheme. One of the calculation methods is based on the correlation function tensor of excitons renormalizing the exciton-photon interaction in the finite system, but this method cannot provide neither the photon-like modes nor photon-like polariton ones. In order to obtain all the exciton-photon coupled modes in the system, we intuitively introduce another calculation method based on the dispersion relation and the self-sustaining condition. This intuitive method actually reproduces the results of the correlation function method, and also provides the photon-like modes and photon-like polariton ones, i.e., all the exciton-photon coupled modes can be obtained. Compared to the same kind of method in our previous letter,[18] the present method can consider the spatial dispersion due to the center-of-mass motion of excitons by using ABCs in the self-sustaining condition. Further, we discussed not only the crossover of the radiative decay rate but also the resonance frequency of the exciton-photon coupled modes, and the general properties were also obtained. Such detailed analysis of the exciton-photon coupled modes in finite systems is important in the experimental verification of the crossover, and also useful when we propose suitable material structures for strong and rapid nonlinear optical responses.

Acknowledgments

The authors are grateful to H. Ajiki for helpful discussions. This work was partially supported by the Japan

Society for the Promotion of Science (JSPS); a Grant-in-Aid for Creative Science Research, 17GS1204, 2005; and a Grant-in-Aid for JSPS Research Fellows.

* Electronic address: motoaki.bamba@univ-paris-diderot.fr
† Present address: Laboratoire MPQ, Université Paris 7 and CNRS, Case 7021, Bâtiment Condorcet, 75205 Paris, France

[1] P. Borri, W. Langbein, S. Schneider, U. Woggon, R. L. Sellin, D. Ouyang, and D. Bimberg, Phys. Rev. Lett. **87**, 157401 (2001).
[2] D. Birkedal, K. Leosson, and J. M. Hvam, Phys. Rev. Lett. **87**, 227401 (2001).
[3] P. Borri, W. Langbein, U. Woggon, V. Stavarache, D. Reuter, and A. D. Wieck, Phys. Rev. B **71**, 115328 (2005).
[4] J. Ishi-Hayase, K. Akahane, N. Yamamoto, M. Sasaki, M. Kujiraoka, and K. Ema, Appl. Phys. Lett. **88**, 261907 (2006).
[5] Y. C. Lee and P. S. Lee, Phys. Rev. B **10**, 344 (1974).
[6] T. Takagahara, Phys. Rev. B **36**, 9293 (1987).
[7] E. Hanamura, Phys. Rev. B **37**, 1273 (1988).
[8] E. Hanamura, Phys. Rev. B **38**, 1228 (1988).
[9] A. Nakamura, H. Yamada, and T. Tokizaki, Phys. Rev. B **40**, 8585 (1989).
[10] T. Itoh, T. Ikehara, and Y. Iwabuchi, J. Lumin. **45**, 29 (1990).
[11] J. Knoester, Phys. Rev. Lett. **68**, 654 (1992).
[12] T. Takagahara, Phys. Rev. B **47**, 16639 (1993).
[13] G. Björk, S. Pau, J. M. Jacobson, H. Cao, and Y. Yamamoto, Phys. Rev. B **52**, 17310 (1995).
[14] V. M. Agranovich, D. M. Basko, and O. A. Dubovsky, J. Chem. Phys. **106**, 3896 (1997).
[15] H. Ajiki, J. Lumin. **94-95**, 173 (2001).
[16] H. Ajiki, T. Tsuji, K. Kawano, and K. Cho, Phys. Rev. B **66**, 245322 (2002).
[17] N. I. Nikolaev, A. Smith, and A. L. Ivanov, J. Phys.: Condens. Matter **16**, S3703 (2004).
[18] M. Bamba and H. Ishihara, J. Phys. Soc. Jpn. **78**, 043701 (2009).
[19] Y. Kayanuma, Phys. Rev. B **38**, 9797 (1988).
[20] Y.-N. Chen and D.-S. Chuu, Phys. Rev. B **61**, 10815 (2000).
[21] H. Ishihara, K. Cho, K. Akiyama, N. Tomita, and T. Isu, phys. status solidi (a) **190**, 849 (2002).
[22] H. Ishihara, J. Kishimoto, and K. Sugihara, J. Lumin. **108**, 343 (2004).
[23] A. Syouji, B. P. Zhang, Y. Segawa, J. Kishimoto, H. Ishihara, and K. Cho, Phys. Rev. Lett. **92**, 257401 (2004).
[24] M. Ichimiya, M. Ashida, H. Yasuda, H. Ishihara, and T. Itoh, phys. status solidi (b) **243**, 3800 (2006).
[25] D. K. Shuh, R. S. Williams, Y. Segawa, J.-i. Kusano, Y. Aoyagi, and S. Namba, Phys. Rev. B **44**, 5827 (1991).
[26] M. Nakayama, S. Wakaiki, K. Mizoguchi, D. Kim, H. Ichida, and Y. Kanematsu, phys. status solidi (c) **3**, 3464 (2006).
[27] P. Meystre and M. Sargent III, *Elements of Quantum Optics* (Springer-Verlag, Berlin, 1999), chap. 18, pp. 377–390, 3rd ed.
[28] W. C. Tait, Phys. Rev. B **5**, 648 (1972).
[29] G. Battaglia, A. Quattropani, and P. Schwendimann, Phys. Rev. B **34**, 8258 (1986).
[30] C. Creatore and A. L. Ivanov, Phys. Rev. B **77**, 075324 (2008).
[31] A. Tredicucci, Y. Chen, F. Bassani, J. Massies, C. Deparis, and G. Neu, Phys. Rev. B **47**, 10348 (1993).
[32] Z. K. Tang, A. Yanase, Y. Segawa, N. Matsuura, and K. Cho, Phys. Rev. B **52**, 2640 (1995).
[33] G. Göger, M. Betz, A. Leitenstorfer, M. Bichler, W. Wegscheider, and G. Abstreiter, Phys. Rev. Lett. **84**, 5812 (2000).
[34] M. Betz, G. Göger, A. Leitenstorfer, M. Bichler, G. Abstreiter, and W. Wegscheider, Phys. Rev. B **65**, 085314 (2002).
[35] H. Ishihara, K. Cho, K. Akiyama, N. Tomita, Y. Nomura, and T. Isu, Phys. Rev. Lett. **89**, 017402 (2002).
[36] K. Akiyama, N. Tomita, Y. Nomura, and T. Isu, Appl. Phys. Lett. **75**, 475 (1999).
[37] K. Cho, *Optical Response of Nanostructures: Microscopic Nonlocal Theory*, (Springer-Verlag, Berlin, 2003).
[38] S. I. Pekar, Zh. Eksp. Teor. Fiz. **33**, 1022 (1957).
[39] V. M. Agranovich and V. L. Ginzburg, *Crystal Optics with Spatial Dispersion, and Excitons*, vol. 42 of *Springer Series in Solid-State Sciences* (Springer-Verlag, Berlin, 1984), second corrected and updated ed.
[40] B. Huttner and S. M. Barnett, Phys. Rev. A **46**, 4306 (1992).
[41] L. Knöll, S. Scheel, and D.-G. Welsch, in *Coherence and Statistics of Photons and Atoms*, edited by J. Peřina (Wiley, New York, 2001), chap. 1, pp. 1–64.
[42] M. Bamba and H. Ishihara, Phys. Rev. B **78**, 085109 (2008).
[43] A. A. Abrikosov, L. P. Gorkov, and I. E. Dzyaloshinski, *Methods of Quantum Field Theory in Statistical Physics* (Dover, New York, 1975), revised English ed.
[44] W. C. Chew, *Waves and Fields in Inhomogeneous Media*, (IEEE, New York, 1995), reprint ed.
[45] R. Zeyher, J. L. Birman, and W. Brenig, Phys. Rev. B **6**, 4613 (1972).